Restudy of the color-allowed two-body nonleptonic decays of bottom baryons Ξ_b and Ω_b supported by hadron spectroscopy

Yu-Shuai Li[1,2,†] and Xiang Liu[1,2,3,*]

[1]*School of Physical Science and Technology, Lanzhou University, Lanzhou 730000, China*
[2]*Research Center for Hadron and CSR Physics, Lanzhou University and Institute of Modern Physics of CAS, Lanzhou 730000, China*
[3]*Lanzhou Center for Theoretical Physics, Key Laboratory of Theoretical Physics of Gansu Province, and Frontier Science Center for Rare Isotopes, Lanzhou University, Lanzhou 730000, China*

(Received 7 December 2021; accepted 23 December 2021; published 6 January 2022)

In this work, we calculate the branching ratios of the color-allowed two-body nonleptonic decays of the bottom baryons, which include the $\Xi_b \to \Xi_c^{(*)}$ and $\Omega_b \to \Omega_c^{(*)}$ weak transitions by emitting a pseudoscalar meson (π^-, K^-, D^-, and D_s^-) or a vector meson (ρ^-, K^{*-}, D^{*-}, and D_s^{*-}). For achieving this aim, we adopt the three-body light-front quark model with the support of hadron spectroscopy, where the spatial wave functions of these heavy baryons involved in these weak decays are obtained by a semirelativistic potential model associated with the Gaussian expansion method. Our results show that these decays with the π^-, ρ^-, and $D_s^{(*)-}$-emitted mode have considerable widths, which could be accessible at the ongoing LHCb and Belle II experiments.

DOI: 10.1103/PhysRevD.105.013003

I. INTRODUCTION

The investigation of bottom baryon weak decay has aroused the attentions from both theorist and experimentalist. It is not only an important approach to deepen our understanding to the dynamics of the weak transition, but also is the crucial step of searching for new physics beyond the Standard Model (SM).

Taking this opportunity, we want to introduce several recent progresses. As we know, the lepton flavor universality (LFU) violation has been examined in various $b \to c$ weak transitions [1–7] in the past decade. The measurement of the ratio $R_{D^{(*)}} = \mathcal{B}(B \to D^{(*)}\tau\nu_\tau)/\mathcal{B}(B \to D^{(*)}e(\mu)\nu_{e(\mu)})$ [1–7] shows the discrepancy with the prediction of the SM [8], which indicates the possible evidence of new physics. Inspired by the anomalies of $R_{D^{(*)}}$ existing in the $b \to c$ weak transitions, it is interesting to study the corresponding ratios for the bottom baryon weak decays like $\Xi_b \to \Xi_c \ell^- \nu_\ell$ and $\Omega_b \to \Omega_c \ell^- \nu_\ell$, where the key point is to calculate the form factors involved in the corresponding weak transition of the bottom baryon into the charmed baryon. For the nonleptonic decays of the bottom baryon, a series of intriguing measurements were performed, which include the observation of charmful and charmless modes [9–12], the discovery of the hidden-charm pentaquark states $P_c(4312)$, $P_c(4380)$, $P_c(4440)$, and $P_c(4457)$ in the $\Lambda_b \to J/\psi p K$ process [13,14], and $P_{cs}(4459)$ in the $\Xi_b \to J/\psi \Lambda K$ process [15]. These efforts make us gain a deeper understanding of the dynamics involved in the heavy-flavor baryon weak decays.

Although great progress had been made, continuing to explore new allowed decay modes of the bottom baryons is a research issue full of opportunity [see the Particle Data Group (PDG) [12] for learning the present experimental status]. With the accumulation of experimental data, the LHCb experiment shows its potential to explore the allowed decays of the bottom baryons like the Ξ_b and Ω_b states, which is still missing in the PDG. Besides, with the KEKB upgrading to the SuperKEKB, the center-of-mass energy of the e^+e^- collision may reach up to 11.24 GeV. The ongoing Belle II [16] should be a potential experiment to perform the study on the bottom-flavor physics. Facing this exciting status, we have reason to believe that it is suitable time to investigate the two-body nonleptonic decays of the Ξ_b and Ω_b baryons, which is the main task of this work.

The bottom baryon weak decays have been widely studied by various approaches including the quark models [17–24], the flavor symmetry method [25], the light-front approach [25–30], and the quantum chromodynamics (QCD) sum rules [31–34]. For these theoretical studies,

*Corresponding author.
xiangliu@lzu.edu.cn
†liysh20@lzu.edu.cn

how to estimate the form factors of the weak transition is the key issue. Additionally, for the bottom baryon weak decays, how to optimize the three-body problem is also a challenge. Usually, the quark-diquark scheme as an approximate treatment was widely used in previous theoretical works [25–29,35]. And the spatial wave functions of these hadrons involved in the bottom baryon weak decays are approximately taken as a simple harmonic oscillator wave function, which makes the results dependent on the parameter of the harmonic oscillator wave function. For avoiding the uncertainty from these approximate treatments mentioned above, in this work we calculate the weak transition form factors of the $\Xi_b \to \Xi_c^{(*)}$ and $\Omega_b \to \Omega_c^{(*)}$ transitions with emitting a pseudoscalar meson (π^-, K^-, D^-, and D_s^-) or a vector meson (ρ^-, K^{*-}, D^{*-} and D_s^{*-}) in the three-body light-front quark model. Here, $\Xi_c^{(*)}$ denotes the ground state Ξ_c or its first radial excited state $\Xi_c(2970)$, while $\Omega_c^{(*)}$ represents the ground state Ω_c or its first radial excited state $\Omega_c(2S)$. In the realistic calculation, we take the numerical spatial wave functions of these involved bottom and charmed baryons as input, where the semirelativistic potential model [30,36] associated with the Gaussian expansion method (GEM) [37–40] is adopted. By fitting the mass spectrum of these observed bottom and charmed baryons, the parameters of the adopted semirelativistic potential model can be fixed. Comparing with former approximation of taking a simple harmonic oscillator wave function [25–29,35], the treatment given in this work can avoid the uncertainties resulting from the selection of the spatial wave function of the heavy baryon. Thus, the color-allowed two-body nonleptonic decays of bottom baryons Ξ_b and Ω_b with the support of hadron spectroscopy as a development. In the following sections, more details will be illustrated.

This paper is organized as follows. After the introduction, the formula of the form factors of the weak transitions $\Xi_b \to \Xi_c^{(*)}$ and $\Omega_b \to \Omega_c^{(*)}$ is given in Sec. II. For getting the numerical spatial wave functions of these involved heavy baryons, we introduce the adopted semirelativistic potential model and GEM. With these results as input, the calculated concerned form factors are displayed. In Sec. III, we study the color-allowed two-body nonleptonic decays with emitting a pseudoscalar meson (π^-, K^-, D^-, and D_s^-) or vector meson (ρ^-, K^{*-}, D^{*-}, and D_s^{*-}) in the naïve factorization assumption. Finally, the paper ends with a short summary.

II. THE TRANSITION FORM FACTORS OF THE BOTTOM BARYON TO THE CHARMED BARYON

In this section, we briefly introduce how to calculate the form factors discussed in this work. Given that the quarks are confined in hadron, the weak transition matrix element cannot be calculated in the framework of perturbative QCD. Usually, the weak transition matrix element can be parametrized in terms of a series of dimensionless form factors [28,30]

$$\begin{aligned}\langle \mathcal{B}_c(1/2^+)(P',J_z')|\bar{c}\gamma^\mu(1-\gamma_5)b|\mathcal{B}_b(1/2^+)(P,J_z)\rangle &= \bar{u}(P',J_z')\left[f_1^V(q^2)\gamma^\mu + i\frac{f_2^V(q^2)}{M}\sigma^{\mu\nu}q_\nu + \frac{f_3^V(q^2)}{M}q^\mu \right. \\ &\left. -\left(g_1^A(q^2)\gamma^\mu + i\frac{g_2^A(q^2)}{M}\sigma^{\mu\nu}q_\nu + \frac{g_3^A(q^2)}{M}q^\mu\right)\gamma_5\right]u(P,J_z)\end{aligned} \tag{2.1}$$

for the transitions of the bottom baryon to the charmed baryon. Here, $M(P)$ and $M'(P')$ are the mass (four-momentum) for the initial and final baryons, respectively, $\sigma^{\mu\nu} = i[\gamma^\mu,\gamma^\nu]/2$, and $q = P - P'$ denotes the transferred momentum between the initial and final baryons.

The vertex function of a single heavy-flavor baryon $\mathcal{B}_Q$ ($Q = b$, c) with the spin $J = 1/2$ and the momentum P is

$$\begin{aligned}|\mathcal{B}_Q(P,J,J_z)\rangle = \int \frac{d^3\tilde{p}_1}{2(2\pi)^3}\frac{d^3\tilde{p}_2}{2(2\pi)^3}\frac{d^3\tilde{p}_3}{2(2\pi)^3}2(2\pi)^3 &\times \sum_{\lambda_1,\lambda_2,\lambda_3}\Psi^{J,J_z}(\tilde{p}_i,\lambda_i)C^{\alpha\beta\gamma}\delta^3(\tilde{\bar{P}}-\tilde{p}_1-\tilde{p}_2-\tilde{p}_3) \\ &\times F_{nnQ}|n_\alpha(\tilde{p}_1,\lambda_1)\rangle|n_\beta(\tilde{p}_2,\lambda_2)\rangle|Q_\gamma(\tilde{p}_3,\lambda_3)\rangle.\end{aligned} \tag{2.2}$$

Here, $n = u$, d, s is the light-flavor quark, $C^{\alpha\beta\gamma}$ and F_{nnQ} represent the color and flavor factors, and λ_i and p_i ($i = 1, 2, 3$) are the helicities and light-front momenta of the on-mass-shell quarks, respectively, defined as

$$\tilde{p}_i = (p_i^+, p_{i\perp}), \quad p_i^+ = p_i^0 + p_i^3, \quad p_{i\perp} = (p_i^1, p_i^2). \tag{2.3}$$

As suggested in Ref. [41], the spin and spatial wave functions for $\mathcal{B}_Q(\bar{3}_f)$ and $\mathcal{B}_Q(6_f)$ with the spin-parity quantum number $J^P = 1/2^+$ are written as

$$\begin{aligned}\Psi^{J,J_z}(\tilde{p}_i,\lambda_i) &= A_0\bar{u}(p_1,\lambda_1)[(\bar{\not{P}}+M_0)\gamma_5]v(p_2,\lambda_2) \\ &\times \bar{u}_Q(p_3,\lambda_3)u(\bar{P},J,J_z)\phi(x_i,k_{i\perp}), \\ \Psi^{J,J_z}(\tilde{p}_i,\lambda_i) &= A_1\bar{u}(p_1,\lambda_1)[(\bar{\not{P}}+M_0)\gamma_{\perp\alpha}]v(p_2,\lambda_2) \\ &\times \bar{u}_Q(p_3,\lambda_3)\gamma_\perp^\alpha\gamma_5 u(\bar{P},J,J_z)\phi(x_i,k_{i\perp}),\end{aligned} \tag{2.4}$$

with

$$A_0 = \sqrt{3}A_1 = \frac{1}{\sqrt{16\bar{P}^+M_0^3(e_1+m_1)(e_2+m_2)(e_3+m_3)}}$$

representing the normalization factor [28].

In the framework of the three-body light-front quark model, the general expressions are written as [28,30]

$$\langle \mathcal{B}_c^{(*)}(\bar{3}_f, 1/2^+)(\bar{P}', J_z')|\bar{c}\gamma^\mu(1-\gamma_5)b|\mathcal{B}_b(\bar{3}_f, 1/2^+)(\bar{P}, J_z)\rangle$$
$$= \int \left(\frac{dx_1 d^2\vec{k}_{1\perp}}{2(2\pi)^3}\right)\left(\frac{dx_2 d^2\vec{k}_{2\perp}}{2(2\pi)^3}\right)\frac{\phi(x_i,\vec{k}_{i\perp})\phi^*(x_i',\vec{k}_{i\perp}{}')}{16\sqrt{x_3 x_3' {M_0}^3 {M_0'}^3}}\frac{\mathrm{Tr}[(\bar{\not{P}}'+M_0')\gamma_5(\not{p}_1+m_1)(\bar{\not{P}}+M_0)\gamma_5(\not{p}_2-m_2)]}{\sqrt{(e_1+m_1)(e_2+m_2)(e_3+m_3)(e_1'+m_1')(e_2'+m_2')(e_3'+m_3')}}$$
$$\times \bar{u}(\bar{P}', J_z')(\not{p}_3{}'+m_3')\gamma^\mu(1-\gamma_5)(\not{p}_3+m_3)u(\bar{P}, J_z), \tag{2.5}$$

$$\langle \mathcal{B}_c^{(*)}(6_f, 1/2^+)(\bar{P}', J_z')|\bar{c}\gamma^\mu(1-\gamma_5)b|\mathcal{B}_b(6_f, 1/2^+)(\bar{P}, J_z)\rangle$$
$$= \int \left(\frac{dx_1 d^2\vec{k}_{1\perp}}{2(2\pi)^3}\right)\left(\frac{dx_2 d^2\vec{k}_{2\perp}}{2(2\pi)^3}\right)\frac{\phi(x_i,\vec{k}_{i\perp})\phi^*(x_i',\vec{k}_{i\perp}{}')}{48\sqrt{x_3 x_3' {M_0}^3 {M_0'}^3}}\frac{\mathrm{Tr}[\gamma_\perp^\alpha(\bar{\not{P}}'+M_0')(\not{p}_1+m_1)(\bar{\not{P}}+M_0)\gamma_\perp^\beta(\not{p}_2-m_2)]}{\sqrt{(e_1+m_1)(e_2+m_2)(e_3+m_3)(e_1'+m_1')(e_2'+m_2')(e_3'+m_3')}}$$
$$\times \bar{u}(\bar{P}', J_z')\gamma_{\perp\alpha}\gamma_5(\not{p}_3{}'+m_3')\gamma^\mu(1-\gamma_5)(\not{p}_3+m_3)\gamma_{\perp\beta}\gamma_5 u(\bar{P}, J_z), \tag{2.6}$$

for the $\mathcal{B}_b(\bar{3}_f) \to \mathcal{B}_c(\bar{3}_f)$ and $\mathcal{B}_b(6_f) \to \mathcal{B}_c(6_f)$ transitions, respectively. Here, $\bar{P} = p_1 + p_2 + p_3$ and $\bar{P}' = p_1 + p_2 + p_3'$ are the light-front momenta for initial and final baryons, respectively, considering $p_1 = p_1'$ and $p_2 = p_2'$ in the spectator scheme, while ϕ and ϕ^* represent the spatial wave functions for the initial bottom baryon and the final charmed baryon, respectively. In the previous references [25–29,35], the wave functions for baryon are usually treated as a simple harmonic oscillator forms with the oscillator parameter β, which results in the β dependence of the result. For avoiding this uncertainty, in this work, we adopt the numerical spatial wave functions for these involved baryons calculated by solving the three-body Schrödinger equation with the semirelativistic quark model.

To calculate the form factors defined in Eq. (2.1) from Eqs. (2.5)–(2.6), V^+, A^+, $\vec{q}_\perp\cdot\vec{V}$, $\vec{q}_\perp\cdot\vec{A}$, $\vec{n}_\perp\cdot\vec{V}$, and $\vec{n}_\perp\cdot\vec{A}$ are applied within a special gauge $q^+ = 0$. The details can be found in Ref. [27]. Finally, the form factors are expressed as [30]

$$f_1^V(q^2) = \int \mathcal{D}S_0 \frac{1}{8\bar{P}^+\bar{P}'^+}\mathrm{Tr}[(\bar{\not{P}}+M_0)\gamma^+(\bar{\not{P}}'+M_0')(\not{p}_3{}'+m_3')\gamma^+(\not{p}_3+m_3)],$$
$$f_2^V(q^2) = \int \mathcal{D}S_0 \frac{iM}{8\bar{P}^+\bar{P}'^+q^2}\mathrm{Tr}[(\bar{\not{P}}+M_0)\sigma^{+\mu}q_\mu(\bar{\not{P}}'+M_0')(\not{p}_3{}'+m_3')\gamma^+(\not{p}_3+m_3)],$$
$$f_3^V(q^2) = \frac{M}{M+M'}\left(f_1^V(q^2)\left(1-\frac{2\bar{P}\cdot q}{q^2}\right)+\int\frac{\mathcal{D}S_0}{4\sqrt{\bar{P}^+\bar{P}'^+}q^2}\mathrm{Tr}[(\bar{\not{P}}+M_0)\gamma^+(\bar{\not{P}}'+M_0')(\not{p}_3{}'+m_3')\not{q}\not{p}_3+m_3)]\right),$$
$$g_1^A(q^2) = \int \mathcal{D}S_0 \frac{1}{8\bar{P}^+\bar{P}'^+}\mathrm{Tr}[(\bar{\not{P}}+M_0)\gamma^+\gamma_5(\bar{\not{P}}'+M_0')(\not{p}_3{}'+m_3')\gamma^+\gamma_5(\not{p}_3+m_3)],$$
$$g_2^A(q^2) = \int \mathcal{D}S_0 \frac{-iM}{8\bar{P}^+\bar{P}'^+q^2}\mathrm{Tr}[(\bar{\not{P}}+M_0)\sigma^{+\mu}q_\mu\gamma_5(\bar{\not{P}}'+M_0')(\not{p}_3{}'+m_3')\gamma^+\gamma_5(\not{p}_3+m_3)],$$
$$g_3^A(q^2) = \frac{M}{M-M'}\left(g_1^A(q^2)\left(-1+\frac{2\bar{P}\cdot q}{q^2}\right)+\int\frac{-\mathcal{D}S_0}{4\sqrt{\bar{P}^+\bar{P}'^+}q^2}\mathrm{Tr}[(\bar{\not{P}}+M_0)\gamma^+\gamma_5(\bar{\not{P}}'+M_0')(\not{p}_3{}'+m_3')\not{q}\gamma_5(\not{p}_3+m_3)]\right),$$
$$\mathcal{D}S_0 = \frac{dx_1 d^2\vec{k}_{1\perp}dx_2 d^2\vec{k}_{2\perp}}{2(2\pi)^3 2(2\pi)^3}\frac{\phi^*(x_i',\vec{k}_{i\perp}{}')\phi(x_i,\vec{k}_{i\perp})}{16\sqrt{x_3 x_3' M_0^3 {M_0'}^3}}\frac{\mathrm{Tr}[(\bar{\not{P}}'-M_0')\gamma_5(\not{p}_1+m_1)(\bar{\not{P}}+M_0)\gamma_5(\not{p}_2-m_2)]}{\sqrt{(e_1+m_1)(e_2+m_2)(e_3+m_3)(e_1'+m_1')(e_2+m_2')(e_3'+m_3')}}, \tag{2.7}$$

and

$$
\begin{aligned}
f_1^V(q^2) &= \int \mathcal{D}S_1 \frac{1}{8\bar{P}^+\bar{P}'^+}\mathrm{Tr}[(\bar{\not{P}}+M_0)\gamma^+(\bar{\not{P}}'+M_0')\gamma_{\perp\alpha}\gamma_5(\not{p}_3'+m_3')\gamma^+(\not{p}_3+m_3)\gamma_{\perp\beta}\gamma_5],\\
f_2^V(q^2) &= \int \mathcal{D}S_1 \frac{iM}{8\bar{P}^+\bar{P}'^+q^2}\mathrm{Tr}[(\bar{\not{P}}+M_0)\sigma^{+\mu}q_\mu(\bar{\not{P}}'+M_0')\gamma_{\perp\alpha}\gamma_5(\not{p}_3'+m_3')\gamma^+(\not{p}_3+m_3)\gamma_{\perp\beta}\gamma_5],\\
f_3^V(q^2) &= \frac{M}{M+M'}\left(f_1^V(q^2)\left(1-\frac{2\bar{P}\cdot q}{q^2}\right)+\int\frac{\mathcal{D}S_1}{4\sqrt{\bar{P}^+\bar{P}'^+}q^2}\mathrm{Tr}[(\bar{\not{P}}+M_0)\gamma^+(\bar{\not{P}}'+M_0')\gamma_{\perp\alpha}\gamma_5(\not{p}_3'+m_3')\not{q}\not{p}_3+m_3)\gamma_{\perp\beta}\gamma_5]\right),\\
g_1^A(q^2) &= \int \mathcal{D}S_1 \frac{1}{8\bar{P}^+\bar{P}'^+}\mathrm{Tr}[(\bar{\not{P}}+M_0)\gamma^+\gamma_5(\bar{\not{P}}'+M_0')\gamma_{\perp\alpha}\gamma_5(\not{p}_3'+m_3')\gamma^+\gamma_5(\not{p}_3+m_3)\gamma_{\perp\beta}\gamma_5],\\
g_2^A(q^2) &= \int \mathcal{D}S_1 \frac{-iM}{8\bar{P}^+\bar{P}'^+q^2}\mathrm{Tr}[(\bar{\not{P}}+M_0)\sigma^{+\mu}q_\mu\gamma_5(\bar{\not{P}}'+M_0')\gamma_{\perp\alpha}\gamma_5(\not{p}_3'+m_3')\gamma^+\gamma_5(\not{p}_3+m_3)\gamma_{\perp\beta}\gamma_5],\\
g_3^A(q^2) &= \frac{M}{M-M'}\left(g_1^A(q^2)\left(-1+\frac{2\bar{P}\cdot q}{q^2}\right)\right.\\
&\quad\left.+\int\frac{-\mathcal{D}S_1}{4\sqrt{\bar{P}^+\bar{P}'^+}q^2}\mathrm{Tr}[(\bar{\not{P}}+M_0)\gamma^+\gamma_5(\bar{\not{P}}'+M_0')\gamma_{\perp\alpha}\gamma_5(\not{p}_3'+m_3')\not{q}\gamma_5(\not{p}_3+m_3)\gamma_{\perp\beta}\gamma_5]\right),\\
\mathcal{D}S_1 &= \frac{dx_1d^2\vec{k}_{1\perp}dx_2d^2\vec{k}_{2\perp}}{2(2\pi)^32(2\pi)^3}\frac{\phi^*(x_i',\vec{k}_{i\perp}')\phi(x_i,\vec{k}_{i\perp})}{48\sqrt{x_3x_3'M_0^3M_0'^3}}\frac{\mathrm{Tr}[\gamma_\perp^\alpha(\bar{\not{P}}'+M_0')(\not{p}_1+m_1)(\bar{\not{P}}+M_0)\gamma_\perp^\beta(\not{p}_2-m_2)]}{\sqrt{(e_1+m_1)(e_2+m_2)(e_3+m_3)(e_1'+m_1')(e_2+m_2')(e_3'+m_3')}},
\end{aligned}
\tag{2.8}
$$

for the $\mathcal{B}_b(\bar{3}_f)\to\mathcal{B}_c(\bar{3}_f)$ and $\mathcal{B}_b(6_f)\to\mathcal{B}_c(6_f)$ transitions, respectively.

III. THE SEMIRELATIVISTIC POTENTIAL MODEL FOR CALCULATING BARYON WAVE FUNCTION

In this section, we illustrate how to obtain the concerned spatial wave functions by the semirelativistic quark model with the help of the GEM. Different from the meson system, baryon is a typical three-body system. Thus, its wave function can be extracted by solving the three-body Schrödinger equation. Here, the semirelativistic potentials were given in Refs. [36,42], which are applied to the realistic calculation of this work. The involved Hamiltonian includes [30]

$$
\mathcal{H} = K + \sum_{i<j}(S_{ij}+G_{ij}+V_{ij}^{\mathrm{so(s)}}+V_{ij}^{\mathrm{so(v)}}+V_{ij}^{\mathrm{ten}}+V_{ij}^{\mathrm{con}}),
\tag{3.1}
$$

with K, S, G, $V^{\mathrm{so}(s)}$, $V^{\mathrm{so}(v)}$,V^{tens}, and V^{con} representing the kinetic energy, the spin-independent linear confinement piece, the Coulomb-like potential, the scalar type-spin-orbit interaction, the vector type-spin-orbit interaction, the tensor potential, and the spin-dependent contact potential, respectively. Their concrete expressions are listed here [36,42–44]:

$$
K = \sum_{i=1,2,3}\sqrt{m_i^2+p_i^2},
\tag{3.2}
$$

$$
S_{ij} = -\frac{3}{4}\left(br_{ij}\left[\frac{e^{-\sigma^2r_{ij}^2}}{\sqrt{\pi}\sigma r_{ij}}+\left(1+\frac{1}{2\sigma^2r_{ij}^2}\right)\frac{2}{\sqrt{\pi}}\right.\right.
\left.\left.\times\int_0^{\sigma r_{ij}}e^{-x^2}dx\right]\right)\mathbf{F_i}\cdot\mathbf{F_j}+\frac{c}{3},
\tag{3.3}
$$

$$
G_{ij} = \sum_k\frac{\alpha_k}{r_{ij}}\left[\frac{2}{\sqrt{\pi}}\int_0^{\tau_k r_{ij}}e^{-x^2}dx\right]\mathbf{F_i}\cdot\mathbf{F_j},
\tag{3.4}
$$

for the spin-independent terms with

$$
\sigma^2 = \sigma_0^2\left[\frac{1}{2}+\frac{1}{2}\left(\frac{4m_im_j}{(m_i+m_j)^2}\right)^4+s^2\left(\frac{2m_im_j}{m_i+m_j}\right)^2\right],
\tag{3.5}
$$

and

$$
\begin{aligned}
V_{ij}^{\mathrm{so}(s)} &= -\frac{\mathbf{r_{ij}}\times\mathbf{p_i}\cdot\mathbf{S_i}}{2m_i^2}\frac{1}{r_{ij}}\frac{\partial S_{ij}}{r_{ij}}+\frac{\mathbf{r_{ij}}\times\mathbf{p_j}\cdot\mathbf{S_j}}{2m_j^2}\frac{1}{r_{ij}}\frac{\partial S_{ij}}{\partial r_{ij}},\\
V_{ij}^{\mathrm{so}(v)} &= \frac{\mathbf{r_{ij}}\times\mathbf{p}_i\cdot\mathbf{S_i}}{2m_i^2}\frac{1}{r_{ij}}\frac{\partial G_{ij}}{r_{ij}}-\frac{\mathbf{r_{ij}}\times\mathbf{p_j}\cdot\mathbf{S_j}}{2m_j^2}\frac{1}{r_{ij}}\frac{\partial G_{ij}}{r_{ij}}\\
&\quad-\frac{\mathbf{r_{ij}}\times\mathbf{p_j}\cdot\mathbf{S_i}-\mathbf{r_{ij}}\times\mathbf{p_i}\cdot\mathbf{S_j}}{m_im_j}\frac{1}{r_{ij}}\frac{\partial G_{ij}}{\partial r_{ij}},\\
V_{ij}^{\mathrm{tens}} &= -\frac{1}{m_im_j}\left[(\mathbf{S_i}\cdot\hat{\mathbf{r}}_{\mathbf{ij}})(\mathbf{S_j}\cdot\hat{\mathbf{r}}_{\mathbf{ij}})-\frac{\mathbf{S_i}\cdot\mathbf{S_j}}{3}\right]\\
&\quad\times\left(\frac{\partial^2G_{ij}}{\partial r^2}-\frac{\partial G_{ij}}{r_{ij}\partial r_{ij}}\right),\\
V_{ij}^{\mathrm{con}} &= \frac{2\mathbf{S_i}\cdot\mathbf{S_j}}{3m_im_j}\nabla^2G_{ij},
\end{aligned}
$$

for the spin-dependent terms, where m_i and m_j are the masses of quark i and j, respectively. And, we take $\langle \mathbf{F_i} \cdot \mathbf{F_j} \rangle = -2/3$ for quark-quark interaction.

In the following, a general potential which relies on the center-of-mass of interacting quarks and momentum are made up for the loss of relativistic effects in the nonrelativistic limit [36,42,45–47], that is,

$$G_{ij} \to \left(1+\frac{p^2}{E_iE_j}\right)^{1/2} G_{ij} \left(1+\frac{p^2}{E_iE_j}\right)^{1/2},$$
$$\frac{V_{ij}^k}{m_im_j} \to \left(\frac{m_im_j}{E_iE_j}\right)^{1/2+\epsilon_k} \frac{V_{ij}^k}{m_im_j} \left(\frac{m_im_j}{E_iE_j}\right)^{1/2+\epsilon_k} \tag{3.6}$$

with $E_i = \sqrt{p^2+m_i^2}$, where subscript k was applied to distinguish the contributions from the contact, tensor, vector spin-orbit, and scalar spin-orbit terms. In addition, ϵ_k represents the relevant modification parameters, which are collected in Table I.

The total wave function of the single heavy baryon is composed of color, flavor, spatial, and spin wave functions, i.e.,

$$\Psi_{\mathbf{J},\mathbf{M_J}} = \chi^c \{\chi^s_{\mathbf{S},\mathbf{M_S}} \psi^p_{\mathbf{L},\mathbf{M_L}}\}_{\mathbf{J},\mathbf{M_J}} \psi^f, \tag{3.7}$$

where $\chi^c = (rgb - rbg + gbr - grb + brg - bgr)/\sqrt{6}$ is the color wave function, which is universal for the baryon. For the $\Xi_Q^{(*)}$ baryon, its flavor wave function is $\psi^{\text{flavor}}_{\Xi_Q^{(*)}} = (ns - sn)Q/\sqrt{2}$, while for the $\Omega_Q^{(*)}$ baryon, its flavor wave function denotes $\psi^{\text{flavor}}_{\Omega_Q^{(*)}} = ssQ$, where $Q = b, c$ and $n = u, d$. [1]Besides, $\mathbf{S}$ denotes the total spin and $\mathbf{L}$ is the total orbital angular momentum. $\psi^p_{\mathbf{L},\mathbf{M_L}}$ is the spatial wave function which is composed of ρ mode and λ mode, that is,

$$\psi^p_{\mathbf{L},\mathbf{M_L}}(\vec{\rho},\vec{\lambda}) = \{\phi_{\boldsymbol{l_\rho},\boldsymbol{ml_\rho}}(\vec{\rho})\phi_{\boldsymbol{l_\lambda},\boldsymbol{ml_\lambda}}(\vec{\lambda})\}_{\mathbf{L},\mathbf{M_L}}, \tag{3.8}$$

where the subscripts $\boldsymbol{l_\rho}$ and $\boldsymbol{l_\lambda}$ are the orbital angular momentum quanta for ρ and λ mode, respectively, and the internal Jacobi coordinates are chosen as

[1]A brief introduction about the classification of the single heavy baryons is helpful to the reader to understand how to construct their wave functions. The single heavy baryons with one heavy-flavor quark and two light-flavor quarks belong to the symmetric 6_F or antisymmetric $\bar{3}_F$ flavor representations based on the flavor SU(3) symmetry. The total color-flavor-spin wave functions for the S-wave members must be antisymmetric. Considering the color wave function is antisymmetric invariably, hence the spin of the two light quarks is $S = 1$ for 6_F (e.g., Σ_Q, Ξ'_Q, and Ω_Q) or $S = 0$ for $\bar{3}_F$ (e.g., Λ_Q and Ξ_Q). More details about the classification of the single heavy baryons can be found in Refs. [48,49]. For Ξ'_Q, its flavor wave function is $\psi^{\text{flavor}}_{\Xi'_Q} = (ns + sn)Q/\sqrt{2}$.

TABLE I. The parameters used in the semirelativistic potential model [30].

Parameters	Values	Parameters	Values
m_u (GeV)	0.220	$\epsilon^{so(s)}$	0.448
m_d (GeV)	0.220	$\epsilon^{so(v)}$	−0.062
m_s (GeV)	0.419	ϵ^{tens}	0.379
m_c (GeV)	1.628	ϵ^{con}	−0.142
m_b (GeV)	4.977	σ_0 (GeV)	2.242
b(GeV^2)	0.142	s	0.805
c (GeV)	−0.302		

$$\vec{\rho} = \vec{r}_1 - \vec{r}_2, \qquad \vec{\lambda} = \vec{r}_3 - \frac{m_1\vec{r}_1 + m_2\vec{r}_2}{m_1+m_2}. \tag{3.9}$$

In this work, the Gaussian basis [38–40],

$$\phi^G_{nlm}(\vec{r}) = \phi^G_{nl}(r)Y_{lm}(\hat{r}) = \sqrt{\frac{2^{l+2}(2\nu_n)^{l+3/2}}{\sqrt{\pi}(2l+1)!!}} \lim_{\varepsilon\to 0} \frac{1}{(\nu_n\varepsilon)^l} \sum_{k=1}^{k_{\max}} C_{lm,k} e^{-\nu_n(\vec{r}-\varepsilon\vec{D}_{lm,k})^2}, \tag{3.10}$$

is adopted to expand the spatial wave functions $\phi_{\boldsymbol{l_\rho},\boldsymbol{ml_\rho}}$ and $\phi_{\boldsymbol{l_\lambda},\boldsymbol{ml_\lambda}}$ ($n = 1, 2, \ldots, n_{\max}$). Here, a freedom parameter $n_{\max}$ should be chosen from positive integers, and the Gaussian size parameter ν_n is settled as a geometric progression as

$$\nu_n = 1/r_n^2, \qquad r_n = r_{\min}a^{n-1}, \tag{3.11}$$

with

$$a = \left(\frac{r_{\max}}{r_{\min}}\right)^{\frac{1}{n_{\max}-1}}.$$

Meanwhile, in our calculation the values of $\rho_{\min}$ and $\rho_{\max}$ are chosen as 0.2 and 2.0 fm, respectively, and $n_{\rho_{\max}} = 6$. For λ mode, we also use the same Gaussian sized parameters.

The Rayleigh-Ritz variational principle is used in this work to solve the three-body Schrödinger equation

$$\mathcal{H}\Psi_{\mathbf{J},\mathbf{M_J}} = E\Psi_{\mathbf{J},\mathbf{M_J}}. \tag{3.12}$$

Finally, by solving Schrödinger equation, the masses and wave functions of the baryons are obtained, which are collected in Table II.

As collected in the PDG [12], there are ten states in the Ξ_c family, where the ground states includes Ξ_c^+ and Ξ_c^0 with the quark flavor usc and dsc, respectively. Ξ_c^+ was first reported by SPEC [50], and then confirmed in Ref. [51] by analyzing the $\Xi^-\pi^+\pi^+$ final state, while the neutral one Ξ_c^0 was first discovered by CLEO [52] in the $\Xi^-\pi^+$ mode.

The masses fitted by the PDG are 2467.71 ± 0.23 and 2470.44 ± 0.28 MeV for charged Ξ_c^+ and neutral Ξ_c^0, respectively. And then, the Belle Collaboration found $\Xi_c^+(2970)$ and $\Xi_c^0(2970)$ in the $\Lambda_c^+ K^- \pi^+$ and $\Lambda_c^+ K_S^0 \pi^-$ final states [53], respectively, where the masses of the charged and neutral $\Xi_c(2970)$ states are measured to be 2964.3 ± 1.5 and 2967.1 ± 1.7 MeV, respectively. As indicated by our calculation shown in Table II, the observed $\Xi_c(2970)$ are good candidate of $\Xi_c^*(2S)$. The ground Ω_c state, denoted as $\Omega_c(\frac{1}{2}^+)$, was firstly observed in the $\Xi^- K^- \pi^+ \pi^+$ channel by WA62 [54], and then was confirmed in ARGUS [55] by checking the same mode. Its mass was fitted as 2695.2 ± 1.7 MeV by the PDG. Our result given in Table II indeed supports this assignment since the calculated mass of $\Omega_c(\frac{1}{2}^+)$ is 2.692 GeV consistent with the experimental data. For the $\Omega_c^*(\frac{1}{2}^+)$ state, which is the first radial excitation of $\Omega_c(\frac{1}{2}^+)$, its mass is calculated to be 3.149 GeV.[2]

In Table II, we also collected the numerical spatial wave functions corresponding to these charmed baryons, which will be applied to the following study.

IV. THE FORM FACTORS AND COLOR-ALLOWED TWO-BODY NONLEPTONIC DECAYS

A. The weak transitions form factors

With the input of these obtained numerical wave functions of bottom (see Table II) and charmed baryons, and the expressions of the form factors [see Eqs. (2.7)–(2.8)], we present the numerical results for the weak transition form factors of $\Xi_b \to \Xi_c^{(*)}(1/2^+)$ and $\Omega_b \to \Omega_c^{(*)}(1/2^+)$ processes. Since the expressions of form factors in Eqs. (2.5)–(2.8) are working in the spacelike region ($q^2 < 0$), we need to extend them to the timelike region ($q^2 > 0$). The dipole form [26–28,30]

$$F(q^2) = \frac{F(0)}{(1 - q^2/M^2)[1 - b_1(q^2/M^2) + b_2(q^2/M^2)^2]} \tag{4.1}$$

is applied in this work, where $F(0)$ is the form factor at $q^2 = 0$, b_1, and b_2 are obtained by computing each form factor by Eqs. (2.7)–(2.8) from $q^2 = -q^2_{\rm max}$ to $q^2 = 0$, and fit them by Eq. (4.1).

With the spatial wave functions obtained in the last subsection, we can calculate out the form factors numerically in the framework of the three-body light-front quark model. In this way, all free parameters of the semirelativistic potential model can be fixed by reproducing the mass spectrum of observed heavy baryons. In the previous work [25–29,35] on baryon weak transitions, simple hadronic oscillator wave function with the oscillator parameter β was widely used to simulate the baryon spatial wave function. This treatment makes the results dependent on β value. In this work, our study is supported by hadron spectroscopy. Thus, we can avoid the above uncertainty resulted by the selection of spatial wave functions of heavy baryons involved in these discussed transitions.

The extended form factors of $\Xi_b \to \Xi_c^{(*)}$ are collected in Table III. The q^2 dependence of $f^V_{1,2,3}$ and $g^A_{1,2,3}$ for the $\Xi_b \to \Xi_c$ and $\Xi_b \to \Xi_c(2970)$ transitions are plotted in Fig. 1.

For the $\Xi_b \to \Xi_c$ transition, the corresponding transition matrix element can be rewritten as [27,64,65]

$$\begin{aligned}&\langle \Xi_c(1/2^+)(\nu')|\bar{c}_{\nu'} \Gamma b_\nu|\Xi_b(1/2^+)(\nu)\rangle \\ &= \zeta(\omega)\bar{u}(\nu')\Gamma u(\nu),\end{aligned} \tag{4.2}$$

in the heavy quark limit at the leading order, so the form factors have more simple behaviors as

$$\begin{aligned}f_1^V(q^2) = g_1^A(q^2) = \zeta(\omega), \\ f_2^V = f_3^V = g_2^A = g_3^A = 0,\end{aligned} \tag{4.3}$$

where $\omega = \nu \cdot \nu' = (M^2 + M'^2 - q^2)/(2MM')$ with $\nu' = p'/M'$ and $\nu = p/M$ denoting the four velocities for Ξ_c and Ξ_b, respectively. $\zeta(\omega)$ is the well-known Isgur-Wise function (IWF) and usually expressed as a Taylor series expansion as

$$\zeta(\omega) = 1 - \zeta_1(\omega - 1) + \frac{\zeta_2}{2}(\omega - 1)^2 + \cdots, \tag{4.4}$$

where $\zeta_1 = -\frac{d\zeta(\omega)}{d\omega}|_{\omega=1}$ and $\zeta_2 = \frac{d^2\zeta(\omega)}{d\omega^2}|_{\omega=1}$ are two shape parameters depicting the IWF. The most obvious character is in the point $q^2 = q^2_{\rm max} = (M - M')^2$ (or $\omega = 1$),

[2] In 2017, the LHCb collaboration [56] announced that five narrow excited Ω_c states, $\Omega_c(3000)$, $\Omega_c(3050)$, $\Omega_c(3066)$, $\Omega_c(3090)$, and $\Omega_c(3119)$, were found in the $\Xi_c^- K^+$ invariant mass spectrum. Later, Belle [57] confirmed four narrow excited Ω_c states in the same mode. The spin-parity of these excited strange charmed baryons are not measured yet. In these five excited Ω_c states, the masses of $\Omega_c(3090)$ and $\Omega_c(3119)$ were measured as 3090.0 ± 0.5 and 3119.1 ± 1.0 MeV, respectively. Their structures were discussed by various theoretical approaches [58–63]. Chen *et al.* [58] indicated that $\Omega_c(3119)$ cannot be a $2S$ candidate by performing an analysis of the mass spectrum and decay behavior. Cheng *et al.* [59] assigned $\Omega_c(3090)$ and $\Omega_c(3119)$ as the first radially excited states with $J^P = 1/2^+$ and $3/2^+$, respectively, by the analysis of the Regge trajectories and a direct calculation of the mass via a quark-diquark model. Wang *et al.* [62] proposed that the $\Omega_c(3119)$ favors the $2S$ assignment by a study with a constituent quark model. Agaev *et al.* [61] discussed the favored assignment $\Omega_c(2S)$ state with $J^P = 1/2^+$ and $3/2^+$ for $\Omega_c(3066)$ and $\Omega_c(3119)$ with QCD sum rules. Thus, establishing $\Omega_c^*(\frac{1}{2}^+)$ state is still ongoing. In this work, we adopt the calculated result as mass input of the $\Omega_c^*(\frac{1}{2}^+)$ state.

TABLE II. Spatial wave functions of the concerned Ξ_Q and Ω_Q from the GI model and GEM. It is worth to mention that the masses for the neutral and charged states are degenerate here due to the same masses for u and d quarks. The second column denotes our theoretically prediction, while the third column denotes the experimental data quoted from the PDG [12]. Here, the first value in each row is the masses for the neutral baryon, while the second one is the mass for the charged state. The Gaussian bases (n_ρ, n_λ) listed in the third column are arranged as $[(1,1),(1,2),\ldots,(1,n_{\lambda_{\max}}),(2,1),(2,2),\ldots,(2,n_{\lambda_{\max}}),\ldots,(n_{\rho_{\max}},1),(n_{\rho_{\max}},2),\ldots,(n_{\rho_{\max}},n_{\lambda_{\max}})]$.

Baryon	This work (GeV)	Experiment (MeV)	Eigenvector
$\Xi_b(\frac{1}{2}^+)$	5.804	5791.9 ± 0.5 5797.0 ± 0.6	[−0.017, −0.040, −0.075, 0.002, −0.003, 0.001, −0.033, −0.026, −0.004, −0.009, 0.004, −0.001, 0.005, −0.266, −0.267, 0.013, −0.009, 0.002, 0.008, 0.017, −0.363, −0.041, 0.007, −0.001, −0.006, 0.004, −0.023, −0.079, 0.014, −0.003, 0.002, 0.001, 0.010, 0.007, −0.003, 0.001]
$\Omega_b(\frac{1}{2}^+)$	6.043	6046.1 ± 1.7	[0.002, 0.004, 0.011, −0.006, 0.003, −0.001, 0.075, −0.024, 0.040, 0.002, 0.000, −0.000, −0.034, 0.361, 0.096, 0.002, −0.001, 0.001, −0.009, −0.022, 0.588, −0.002, 0.011, −0.003, 0.009, −0.025, −0.046, 0.101, −0.025, 0.006, −0.002, 0.006, 0.008, −0.013, 0.005, −0.001]
$\Xi_c(\frac{1}{2}^+)$	2.474	$2470.90^{+0.22}_{-0.29}$ $2467.94^{+0.17}_{-0.20}$	[−0.017, −0.027, −0.082, −0.010, −0.001, 0.000, −0.028, −0.032, −0.010, −0.011, 0.004, −0.001, 0.005, −0.192, −0.315, −0.032, −0.000, 0.000, 0.002, 0.037, −0.297, −0.116, 0.020, −0.005, −0.004, −0.002, −0.010, −0.082, 0.010, −0.002, 0.001, 0.002, 0.007, 0.009, −0.003, 0.001]
$\Xi_c^*(\frac{1}{2}^+)$	2.947	$2970.9^{+0.4}_{-0.6}$ $2966.34^{+0.17}_{-1.00}$	[−0.023, −0.072, −0.098, 0.147, −0.012, 0.003, −0.039, −0.081, −0.007, 0.048, −0.004, 0.001, 0.015, −0.390, −0.469, 0.501, −0.049, 0.011, 0.011, 0.013, −0.268, 0.682, −0.023, 0.005, −0.007, −0.005, −0.048, 0.314, 0.056, −0.010, 0.001, 0.006, 0.012, −0.044, 0.005, −0.000]
$\Omega_c(\frac{1}{2}^+)$	2.692	2695.2 ± 1.7	[0.006, −0.003, 0.019, −0.008, 0.004, −0.001, 0.093, −0.027, 0.045, 0.001, 0.002, −0.000, −0.049, 0.351, 0.135, 0.029, −0.010, 0.003, 0.005, −0.078, 0.527, 0.075, −0.002, −0.001, 0.004, −0.001, −0.071, 0.096, −0.021, 0.005, −0.001, 0.000, 0.013, −0.014, 0.005, −0.001]
$\Omega_c^*(\frac{1}{2}^+)$	3.149	–	[0.022, −0.025, 0.042, −0.016, 0.007, −0.002, 0.100, 0.112, −0.022, −0.060, 0.003, −0.000, −0.043, 0.412, 0.494, −0.188, 0.036, −0.008, −0.002, 0.032, 0.068, −0.754, 0.052, −0.011, −0.008, 0.019, −0.076, −0.375, −0.010, 0.000, 0.003, −0.008, 0.021, 0.036, −0.007, 0.001]

$$f_1^V(q^2_{\max}) = g_1^A(q^2_{\max}) = \zeta(1) = 1.$$

It provided one strong restriction for our result. Besides, when comparing our results with the predictions in heavy quark limit (HQL), we can conclude that our results can well match the requirement from heavy quark effective theory, i.e.,

(1) f_1^V and g_1^A are close to each other, and dominate over $f_{2,3}^V$ and $g_{2,3}^A$.
(2) At $q^2 = q^2_{\max}$, $f_1^V(q^2_{\max}) = 1.015$ and $g_1^A(q^2_{\max}) = 0.978$ are very approach to 1.

In addition we also extract the two IWF's shape parameters ξ_1 and ξ_2 in Eq. (4.4) by fitting $\zeta(\omega)$ from $f_1^V(q^2)$ and $g_1^A(q^2)$, respectively. The concrete results and other theoretical predictions are listed in Table IV.

For the $\Xi_b \to \Xi_c(2970)$ transition, the HQL requires $f_1^V = g_1^A = 0$ at $q^2 = q^2_{\max}$ since the wave functions of the low-lying Ξ_b and the radial excited state $\Xi_c^*(2S)$ are

TABLE III. The form factors for the $\Xi_b \to \Xi_c^{(*)}$ transitions in the standard light front quark model. Here, we adopt the form defined in Eq. (4.1) for analyzing these form factors.

	$F(0)$	$F(q^2_{\max})$	b_1	b_2
		$\Xi_b \to \Xi_c$		
f_1^V	0.481	1.015	0.970	0.233
f_2^V	−0.127	−0.312	1.380	0.578
f_3^V	−0.046	−0.097	1.187	0.875
g_1^A	0.471	0.978	0.929	0.226
g_2^A	−0.026	−0.068	1.318	0.122
g_3^A	−0.154	−0.377	1.493	0.947
		$\Xi_b \to \Xi_c(2970)$		
f_1^V	0.214	0.200	−1.146	2.282
f_2^V	−0.072	−0.081	−0.356	1.600
f_3^V	−0.111	−0.221	1.444	0.168
g_1^A	0.204	0.186	−1.269	2.474
g_2^A	−0.087	−0.231	1.867	−0.907
g_3^A	−0.095	−0.113	−0.022	1.687

TABLE IV. Our results for the IWF's shape parameters of the $\Xi_b \to \Xi_c$ transition. The superscripts $[a]$ and $[b]$ in the second and third rows represent the fitting of f_1^V and g_1^A, respectively.

	ζ_1	ζ_2
This work$^{[a]}$	1.97	3.28
This work$^{[b]}$	2.23	4.63
RQM [20]	2.27	7.74

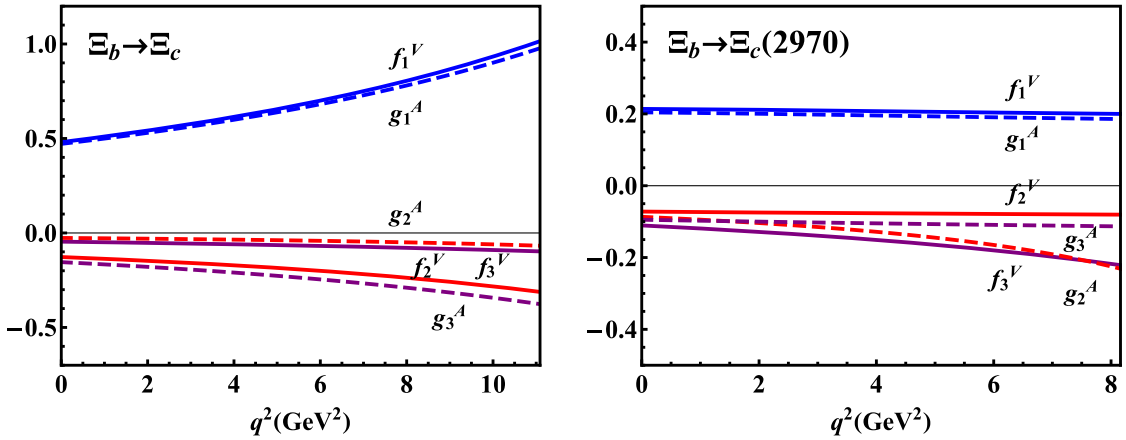

FIG. 1. The q^2 dependence of the form factors $f^V_{1,2,3}(q^2)$ and $g^A_{1,2,3}(q^2)$ for the $\Xi_b \to \Xi_c$ (left) and $\Xi_b \to \Xi_c(2970)$ (right) transitions. Here, the solid and dashed lines represent the vector-type and pseudoscalar-type form factors denoting by the subscripts V and A, respectively, while the blue, red, and purple lines (both solid and dashed lines) represent the ith form factors denoting by the subscripts respectively for each types.

orthogonal [27]. Evidently, our results well embody this prediction according to Fig. 1.

Additionally, the extended form factors of $\Omega_b \to \Omega_c^{(*)}$ are collected in Table V. The q^2 dependence of $f^V_{1,2,3}$ and $g^A_{1,2,3}$ for the $\Omega_b \to \Omega_c$ and $\Omega_b \to \Omega_c(3090)$ transitions are plotted in Fig. 2. For the $\Omega_b \to \Omega_c$ transition, the corresponding transition matrix element can be rewritten as [27,64,65]

$$\langle \Omega_c(1/2^+)(\nu')|\bar{c}_{\nu'}\Gamma b_\nu|\Omega_b(1/2^+)(\nu)\rangle = -\frac{1}{3}(g^{\rho\sigma}\xi_1 - v^\rho v'^\sigma \xi_2)\bar{u}(v')(\gamma_\rho - v'_\rho)\Gamma(\gamma_\sigma - v_\sigma)u(v) \tag{4.5}$$

TABLE V. The form factors for the $\Omega_b \to \Omega_c^{(*)}$ transitions in the standard light front quark model. We use a three parameter form defined in Eq. (4.1) for these form factors.

	$F(0)$	$F(q^2_{\rm max})$	b_1	b_2
		$\Omega_b \to \Omega_c$		
f_1^V	0.493	1.232	1.765	1.272
f_2^V	0.436	1.075	1.658	1.001
f_3^V	−0.255	−0.620	1.628	1.005
g_1^A	−0.161	−0.329	1.053	0.337
g_2^A	0.011	0.018	0.822	1.526
g_3^A	0.055	0.137	1.680	1.052
		$\Omega_b \to \Omega_c(2S)$		
f_1^V	0.180	0.163	−1.135	3.320
f_2^V	0.133	0.107	−1.727	4.270
f_3^V	−0.150	−0.215	0.481	0.239
g_1^A	−0.058	−0.047	−1.701	3.487
g_2^A	0.029	0.053	1.455	0.772
g_3^A	0.023	0.023	−0.671	2.407

in HQL at the leading order. Thus, the form factors in HQL have more simple behaviors as

$$\begin{aligned} f_1^V(q^2_{\rm max}) &= \frac{1}{3} + \frac{1}{3}\frac{M^2 + M'^2}{MM'} = 1.23, \\ f_2^V(q^2_{\rm max}) &= \frac{1}{3}\frac{M + M'}{M'} = 1.08, \\ f_3^V(q^2_{\rm max}) &= -\frac{1}{3}\frac{M - M'}{M'} = -0.41, \\ g_1^A(q^2_{\rm max}) &= -\frac{1}{3}, \\ g_2^A(q^2_{\rm max}) &= g_3^A(q^2_{\rm max}) = 0, \end{aligned} \tag{4.6}$$

at $q^2 = q^2_{\rm max}$ point by substituting the involved masses. Obviously, our results located in the third column of the Table V match well the requirement from the HQL as shown in Eq. (4.6), which can be as a direct test to the HQL.

B. The color-allowed two-body nonleptonic decays

With the preparation of the obtained form factors, we further calculate the color-allowed two-body nonleptonic decays of Ξ_b and Ω with emitting a pseudoscalar meson (π^-, K^-, D^-, and D_s^-) or a vector meson (ρ^-, K^{*-}, D^{*-}, and D_s^{*-}). In this work, the decay rates are investigated by the naïve factorization approach.[3]

[3]The naïve factorization approach works well for the color-allowed dominated processes. But, there exists the case that the color-suppressed and penguin dominated processes can not be explained by the naïve factorization, which may show important nonfactorizable contributions to nonleptonic decays [29]. As indicated in Refs. [26,27,66], the nonfactorizable contributions in bottom baryon nonleptonic decays are considerable comparing with the factorized ones. Since a precise study of nonfactorizable contributions is beyond the scope of the present work, we still adopt the naïve factorization approximation.

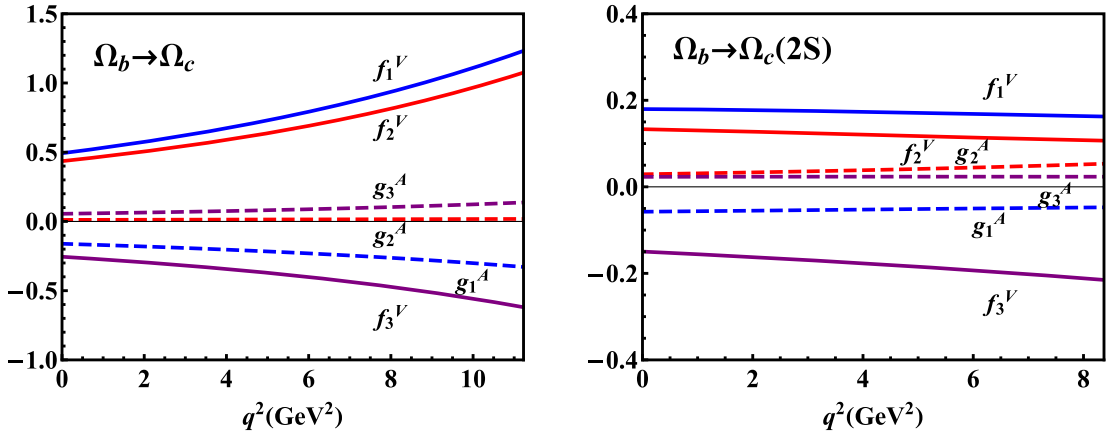

FIG. 2. The q^2 dependence of the form factors $f^V_{1,2,3}(q^2)$ and $g^A_{1,2,3}(q^2)$ for $\Omega_b \to \Omega_c$ (left) and $\Omega_b \to \Omega_c(2S)$ (right) transitions, in which the solid and dashed lines represent the vector or pseudoscalar-types form factors denoting by the subscripts V and A, respectively, while the blue, red, and purple lines (both solid and dashed lines) represent the ith form factors denoting by the subscripts, respectively, for each types.

Generally, in the naïve factorization assumption, the hadronic transition matrix element is factorized into a product of two independent matrix elements [28]

$$\begin{aligned}&\langle \mathcal{B}_c^{(*)}(P', J_z')M^-|\mathcal{H}_{\rm eff}|\mathcal{B}_b(P, J_z)\rangle \\ &= \frac{G_F}{\sqrt{2}} V_{cb}V^*_{qq'}\langle M^-|\bar{q}'\gamma_\mu(1-\gamma_5)q|0\rangle \\ &\quad\times \langle \mathcal{B}_c^{(*)}(P', J_z')|\bar{c}\gamma^\mu(1-\gamma_5)b|\mathcal{B}_b(P, J_z)\rangle, \end{aligned} \tag{4.7}$$

where the meson transition term is given by

$$\langle M|\bar{q}'\gamma_\mu(1-\gamma_5)q|0\rangle = \begin{cases} if_P q_\mu, & M = P \\ if_V \epsilon^*_\mu m_V, & M = V \end{cases}. \tag{4.8}$$

Here, P and V denote pseudoscalar and vector mesons, respectively. The baryon transition term can be obtained by Eq. (2.1). The corresponding Feynman diagram (taking the $\Xi_b^- \to \Xi_c^0 M^-$ as an example here) is displayed in Fig. 3.

Finally the decay width and asymmetry parameter are given by [28]

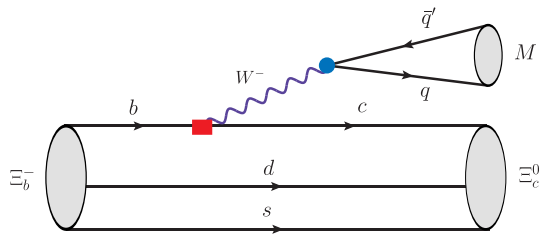

FIG. 3. The diagram for depicting the color-allowed two-body nonleptonic decay $\Xi_b^- \to \Xi_c^0 M^-$ in the tree level.

$$\begin{aligned}\Gamma &= \frac{|p_c|}{8\pi}\left(\frac{(M+M')^2-m^2}{M^2}|A|^2 + \frac{(M-M')^2-m^2}{M^2}|B|^2\right), \\ \alpha &= \frac{2\kappa \mathrm{Re}(A^*B)}{|A|^2+\kappa^2|B|^2}, \end{aligned} \tag{4.9}$$

$$\begin{aligned}\Gamma &= \frac{|p_c|(E'+M')}{4\pi M}\left(2(|S|^2+|P_2|^2)+\frac{E_m^2}{m^2}(|S+D|^2+|P_1|^2)\right), \\ \alpha &= \frac{4m^2\mathrm{Re}(S^*P_2)+2E_m^2\mathrm{Re}(S+D)^*P_1}{2m^2(|S|^2+|P_2|^2)+E_m^2(|S+D|^2+|P_1|^2)}, \end{aligned} \tag{4.10}$$

for the cases involved in the pseudoscalar and vector meson final state, respectively, where p_c is the momentum of the daughter baryon in the rest frame of the parent baryon and $\kappa = |p_c|/(E'+M')$. Besides, $M(E)$ and $M'(E')$ are the masses (energies) of the parent (daughter) baryons, respectively, while $m(E_m)$ denotes the mass (energy) of the meson in the final state.

A and B in Eqs. (4.9) are given by

$$\begin{aligned} A &= \frac{G_F}{\sqrt{2}} V_{cb}V^*_{qq'}a_i f_P (M-M')f_1^V(m^2), \\ B &= -\frac{G_F}{\sqrt{2}} V_{cb}V^*_{qq'}a_i f_P (M+M')g_1^A(m^2), \end{aligned} \tag{4.11}$$

and S, $P_{1,2}$, and D in Eqs. (4.10) are expressed as

$$\begin{aligned} S &= A_1, \\ P_1 &= -\frac{|p_c|}{E_m}\left(\frac{M+M'}{E'+M'}B_1 + MB_2\right), \\ P_2 &= \frac{|p_c|}{E'+M'}B_1, \\ D &= \frac{|p_c|^2}{E_m(E'+M')}(A_1 - MA_2), \end{aligned} \tag{4.12}$$

with

$$A_1 = \frac{G_F}{\sqrt{2}} V_{cb} V^*_{qq'} a_i f_V m_V \left(g_1^A(m^2) + g_2^A(m^2) \frac{M - M'}{M} \right),$$
$$A_2 = \frac{G_F}{\sqrt{2}} V_{cb} V^*_{qq'} a_i f_V m_V (2 g_2^A(m^2)),$$
$$B_1 = \frac{G_F}{\sqrt{2}} V_{cb} V^*_{qq'} a_i f_V m_V \left(f_1^V(m^2) - f_2^V(m^2) \frac{M + M'}{M} \right),$$
$$B_2 = \frac{G_F}{\sqrt{2}} V_{cb} V^*_{qq'} a_i f_V m_V (2 f_2^V(m^2)), \quad (4.13)$$

where $a_1 = c_1 + c_2/N \approx 1.018$ and $a_2 = c_2 + c_1/N \approx 0.170$ [27].

With the naïve factorization, the color-allowed two-body nonleptonic decays by emitting one pseudoscalar meson or vector meson are presented. The lifetimes of $\Xi_b^{-,0}$ and Ω_b^- was reported by the LHCb [67–69] and CDF [70] collaborations. In this work, we use the central values as

$$\tau_{\Xi_b^0} = 1.480 \text{ fs}, \qquad \tau_{\Xi_b^-} = 1.572 \text{ fs}, \qquad \tau_{\Omega_b^-} = 1.65 \text{ fs},$$

averaged by the PDG [12]. Besides, the masses of the concerned baryons are from the GEM calculation and the Cabibbo-Kobayashi-Maskawa matrix elements

$$V_{cb} = 0.0405, \quad V_{ud} = 0.9740, \quad V_{us} = 0.2265,$$
$$V_{cd} = 0.2264, \quad V_{cs} = 0.9732,$$

are taken from the PDG [12]. The decay constants of pseudoscalar and vector mesons include [27,71]

$$f_\pi = 130.2, \quad f_K = 155.6, \quad f_D = 211.9, \quad f_{D_s} = 249.0,$$
$$f_\rho = 216, \quad f_{K^*} = 210, \quad f_{D^*} = 220, \quad f_{D_s^*} = 230,$$

in the unit of MeV.

By substituting our numerical results of the form factors from the three-body light-front quark model and the presented decay parameters into Eqs. (4.9)–(4.10), the branching ratios and asymmetry parameters can be further obtained, which are collected in Tables VI–VII for the $\Xi_b \to \Xi_c^{(*)}$ and $\Omega_b \to \Omega_c^{(*)}$ transitions with emitting a pseudoscalar meson (π^-, K^-, D^-, and D_s^-) or a vector meson (ρ^-, K^{*-}, D^{*-}, and D_s^{*-}), respectively.

In Table VIII, we compare our results of $\mathcal{B}(\Xi_b^{0,-} \to \Xi_c^{+,0} M^-)$ and $\mathcal{B}(\Omega_b^- \to \Omega_c^0 M^-)$ with other theoretical results from the nonrelativistic quark model [21], the relativistic three-quark model [22,23], the light-front quark model [25,27], and the covariant confined quark model [24]. Our results are comparable with those calculated from other approaches. We also notice that the concerned

TABLE VI. The branching ratios and asymmetry parameters of the $\Xi_b \to \Xi_c^{(*)} M$ transitions with M denoting a pseudoscalar or vector meson, where the branching ratios out of or in brackets correspond to the $\Xi_b^0 \to \Xi_c^+$ and $\Xi_b^- \to \Xi_c^0$ transitions, respectively.

Mode	$\mathcal{B}(\times 10^{-3})$	α	Mode	$\mathcal{B}(\times 10^{-3})$	α
$\Xi_b^{0,-} \to \Xi_c^{+,0}\pi^-$	4.04 (4.29)	−1.000	$\Xi_b^{0,-} \to \Xi_c^{+,0}\rho^-$	13.3 (14.1)	−0.792
$\Xi_b^{0,-} \to \Xi_c^{+,0}K^-$	0.31 (0.33)	−1.000	$\Xi_b^{0,-} \to \Xi_c^{+,0}K^{*-}$	0.71 (0.76)	−0.737
$\Xi_b^{0,-} \to \Xi_c^{+,0}D^-$	0.58 (0.62)	−0.983	$\Xi_b^{0,-} \to \Xi_c^{+,0}D^{*-}$	1.51 (1.60)	−0.239
$\Xi_b^{0,-} \to \Xi_c^{+,0}D_s^-$	14.8 (15.7)	−0.978	$\Xi_b^{0,-} \to \Xi_c^{+,0}D_s^{*-}$	32.4 (34.4)	−0.206
$\Xi_b^{0,-} \to \Xi_c^{+,0}(2970)\pi^-$	1.78 (1.89)	−0.999	$\Xi_b^{0,-} \to \Xi_c^{+,0}(2970)\rho^-$	2.78 (2.95)	−0.763
$\Xi_b^{0,-} \to \Xi_c^{+,0}(2970)K^-$	0.04 (0.05)	−0.998	$\Xi_b^{0,-} \to \Xi_c^{+,0}(2970)K^{*-}$	0.09 (0.10)	−0.702
$\Xi_b^{0,-} \to \Xi_c^{+,0}(2970)D^-$	0.04 (0.05)	−0.952	$\Xi_b^{0,-} \to \Xi_c^{+,0}(2970)D^{*-}$	0.12 (0.12)	−0.181
$\Xi_b^{0,-} \to \Xi_c^{+,0}(2970)D_s^-$	1.05 (1.12)	−0.940	$\Xi_b^{0,-} \to \Xi_c^{+,0}(2970)D_s^{*-}$	2.30 (2.45)	−0.148

TABLE VII. The branching rates and asymmetry parameters of $\Omega_b \to \Omega_c^{(*)} M$ transitions with M denoting a pseudoscalar or vector pmeson.

Mode	$\mathcal{B}(\times 10^{-3})$	α	Mode	$\mathcal{B}(\times 10^{-3})$	α
$\Omega_b^- \to \Omega_c^0\pi^-$	2.82	0.59	$\Omega_b^- \to \Omega_c^0\rho^-$	7.92	0.61
$\Omega_b^- \to \Omega_c^0K^-$	0.22	0.58	$\Omega_b^- \to \Omega_c^0K^{*-}$	0.41	0.62
$\Omega_b^- \to \Omega_c^0D^-$	0.52	0.49	$\Omega_b^- \to \Omega_c^0D^{*-}$	0.48	0.69
$\Omega_b^- \to \Omega_c^0D_s^-$	13.5	0.47	$\Omega_b^- \to \Omega_c^0D_s^{*-}$	9.73	0.70
$\Omega_b^- \to \Omega_c^0(2S)\pi^-$	0.30	0.58	$\Omega_b^- \to \Omega_c^0(2S)\rho^-$	0.70	0.60
$\Omega_b^- \to \Omega_c^0(2S)K^-$	0.02	0.57	$\Omega_b^- \to \Omega_c^0(2S)K^{*-}$	0.03	0.60
$\Omega_b^- \to \Omega_c^0(2S)D^-$	0.03	0.45	$\Omega_b^- \to \Omega_c^0(2S)D^{*-}$	0.02	0.65
$\Omega_b^- \to \Omega_c^0(2S)D_s^-$	0.62	0.43	$\Omega_b^- \to \Omega_c^0(2S)D_s^{*-}$	0.36	0.65

TABLE VIII. Comparison of theoretical predictions for $\mathcal{B}(\Xi_b^{0,-} \to \Xi_c^{+,0} M^-)$ and $\mathcal{B}(\Omega_b^- \to \Omega_c^0 M^-)$. Here, all values should be multiplied by a factor of 10^{-3}.

	This work	Cheng [21]	Ivanov *et al.* [22,23]	Zhao [25]	Gutsche *et al.* [24]	Chua [27]
$\Xi_b^{0,-} \to \Xi_c^{+,0}\pi^-$	4.03 (4.29)	4.9 (5.2)	7.08 (10.13)	8.37 (8.93)	–	$3.66^{+2.29}_{-1.59}$ $(3.88^{+2.43}_{-1.69})$
$\Xi_b^{0,-} \to \Xi_c^{+,0}\rho^-$	13.3 (14.1)	–	–	24.0 (25.6)	–	$10.88^{+6.83}_{-4.74}$ $(11.56^{+7.25}_{-5.04})$
$\Xi_b^{0,-} \to \Xi_c^{+,0}K^-$	0.31 (0.33)	–	–	0.667 (0.711)	–	$0.28^{+0.17}_{-0.12}$ $(0.29^{+0.18}_{-0.13})$
$\Xi_b^{0,-} \to \Xi_c^{+,0}K^{*-}$	0.71 (0.76)	–	–	1.23 (1.31)	–	$0.56^{+0.35}_{-0.24}$ $(0.60^{+0.37}_{-0.26})$
$\Xi_b^{0,-} \to \Xi_c^{+,0}D^-$	0.58 (0.62)	–	–	0.949 (1.03)	0.45	$0.43^{+0.29}_{-0.20}$ $(0.45^{+0.31}_{-0.21})$
$\Xi_b^{0,-} \to \Xi_c^{+,0}D^{*-}$	1.51 (1.60)	–	–	1.54 (1.64)	0.95	$0.77^{+0.50}_{-0.35}$ $(0.82^{+0.53}_{-0.37})$
$\Xi_b^{0,-} \to \Xi_c^{+,0}D_s^-$	14.8 (15.7)	14.6	–	24.6 (26.2)	–	$10.87^{+7.51}_{-5.03}$ $(11.54^{+7.98}_{-5.34})$
$\Xi_b^{0,-} \to \Xi_c^{+,0}D_s^{*-}$	32.4 (34.4)	23.1	–	36.5 (39.0)	–	$16.24^{+10.54}_{-7.25}$ $(17.26^{+11.2}_{-7.70})$
$\Omega_b^- \to \Omega_c^0\pi^-$	2.82	4.92	5.81	4.00	1.88	$1.10^{+0.85}_{-0.55}$
$\Omega_b^- \to \Omega_c^0\rho^-$	7.92	12.8	–	10.8	5.43	$3.07^{+2.41}_{-1.53}$
$\Omega_b^- \to \Omega_c^0K^-$	0.22	–	–	0.326	–	$0.08^{+0.07}_{-0.04}$
$\Omega_b^- \to \Omega_c^0K^{*-}$	0.41	–	–	0.544	–	$0.16^{+0.12}_{-0.08}$
$\Omega_b^- \to \Omega_c^0D^-$	0.52	–	–	0.636	–	$0.15^{+0.14}_{-0.08}$
$\Omega_b^- \to \Omega_c^0D^{*-}$	0.48	–	–	0.511	–	$0.16^{+0.13}_{-0.08}$
$\Omega_b^- \to \Omega_c^0D_s^-$	13.5	17.9	–	17.1	–	$4.03^{+3.72}_{-2.21}$
$\Omega_b^- \to \Omega_c^0D_s^{*-}$	9.73	11.5	–	11.7	–	$3.18^{+2.69}_{-1.61}$

transitions with emitting π^-, ρ^-, and $D_s^{(*)-}$ meson have considerable widths, which are worthy to be explored in future experiment like LHCb and Belle II.

V. SUMMARY

With the accumulation of experimental data from LHCb and Belle II [16], experimental exploration of weak decay of the bottom baryons Ξ_b and Ω_b is becoming possible. Facing this opportunity, in this work we study the color-allowed two-body nonleptonic decay of the bottom baryons Ξ_b and Ω_b, i.e., the $\Xi_b \to \Xi_c^{(*)} M$ and $\Omega_b \to \Omega_c^{(*)} M$ decay with emitting a pseudoscalar meson (π^-, K^-, D^-, and D_s^-) or a vector meson (ρ^-, K^{*-}, D^{*-}, and D_s^{*-}).

We adopt the three-body light-front quark model to calculate these form factors depicting these discussed bottom baryon to the charmed baryon transitions under the naïve factorization framework. We also improve the treatment of the spatial wave function of these involved heavy baryons in these decays, where the semirelativistic three-body potential model [30,36] is applied to calculate the numerical spatial wave function of these heavy baryons with the help of the GEM [37–40]. We call that the study of color-allowed two-body nonleptonic decay of bottom baryons Ξ_b and Ω_b is supported by hadron spectroscopy. Our result shows that these color-allowed two-body nonleptonic decays $\Xi_b^{0,-} \to \Xi_c^{(*)+,0}$ and $\Omega_b^- \to \Omega_c^{(*)0}$ with the π^-, ρ^-, and $D_s^{(*)-}$-emitted modes have considerable widths.

We suggest to measure these discussed color-allowed two-body nonleptonic decay of the bottom baryons Ξ_b and Ω_b, which will be good chance for the ongoing LHCb and Belle II experiments.

ACKNOWLEDGMENTS

This work is supported by the China National Funds for Distinguished Young Scientists under Grant No. 11825503, National Key Research and Development Program of China under Contract No. 2020YFA0406400, the 111 Project under Grant No. B20063, the National Natural Science Foundation of China under Grant No. 12047501, and by the Fundamental Research Funds for the Central Universities.

[1] J. P. Lees *et al.* (*BABAR* Collaboration), Evidence for an Excess of $\bar{B} \to D^{(*)}\tau^-\bar{\nu}_\tau$ Decays, Phys. Rev. Lett. **109**, 101802 (2012).

[2] J. P. Lees *et al.* (*BABAR* Collaboration), Measurement of an excess of $\bar{B} \to D^{(*)}\tau^-\bar{\nu}_\tau$ decays and implications for charged Higgs bosons, Phys. Rev. D **88**, 072012 (2013).

[3] M. Huschle *et al.* (Belle Collaboration), Measurement of the branching ratio of $\bar{B} \to D^{(*)}\tau^-\bar{\nu}_\tau$ relative to $\bar{B} \to D^{(*)}\ell^-\bar{\nu}_\ell$ decays with hadronic tagging at Belle, Phys. Rev. D **92**, 072014 (2015).

[4] R. Aaij *et al.* (LHCb Collaboration), Measurement of the Ratio of Branching Fractions $\mathcal{B}(\bar{B}^0 \to D^{*+}\tau^-\bar{\nu}_\tau)/\mathcal{B}(\bar{B}^0 \to D^{*+}\mu^-\bar{\nu}_\mu)$, Phys. Rev. Lett. **115**, 111803 (2015); Erratum, Phys. Rev. Lett. **115**, 159901 (2015).

[5] S. Hirose *et al.* (Belle Collaboration), Measurement of the τ Lepton Polarization and $R(D^*)$ in the Decay $\bar{B} \to D^*\tau^-\bar{\nu}_\tau$, Phys. Rev. Lett. **118**, 211801 (2017).

[6] G. Caria *et al.* (Belle Collaboration), Measurement of $\mathcal{R}(D)$ and $\mathcal{R}(D^*)$ with a Semileptonic Tagging Method, Phys. Rev. Lett. **124**, 161803 (2020).

[7] A. Bazavov *et al.* (Fermilab Lattice and MILC Collaborations), Semileptonic form factors for $B \to D^*\ell\nu$ at nonzero recoil from 2 + 1-flavor lattice QCD, arXiv:2105.14019.

[8] Y. S. Amhis *et al.* (HFLAV Collaboration), Averages of b-hadron, c-hadron, and τ-lepton properties as of 2018, Eur. Phys. J. C **81**, 226 (2021).

[9] T. Aaltonen *et al.* (CDF Collaboration), Observation of New Charmless Decays of Bottom Hadrons, Phys. Rev. Lett. **103**, 031801 (2009).

[10] R. Aaij *et al.* (LHCb Collaboration), Searches for Λ_b^0 and Ξ_b^0 decays to $K_S^0 p\pi^-$ and $K_S^0 pK^-$ final states with first observation of the $\Lambda_b^0 \to K_S^0 p\pi^-$ decay, J. High Energy Phys. 04 (2014) 087.

[11] R. Aaij *et al.* (LHCb Collaboration), Observations of $\Lambda_b^0 \to \Lambda K^+\pi^-$ and $\Lambda_b^0 \to \Lambda K^+K^-$ decays and searches for other Λ_b^0 and Ξ_b^0 decays to $\Lambda h^+h'^-$ final states, J. High Energy Phys. 05 (2016) 081.

[12] P. A. Zyla *et al.* (Particle Data Group), Review of particle physics, Prog. Theor. Exp. Phys. **2020**, 083C01 (2020).

[13] R. Aaij *et al.* (LHCb Collaboration), Observation of $J/\psi p$ Resonances Consistent with Pentaquark States in $\Lambda_b^0 \to J/\psi K^- p$ Decays, Phys. Rev. Lett. **115**, 072001 (2015).

[14] R. Aaij *et al.* (LHCb Collaboration), Observation of a Narrow Pentaquark State, $P_c(4312)^+$, and of Two-Peak Structure of the $P_c(4450)^+$, Phys. Rev. Lett. **122**, 222001 (2019).

[15] R. Aaij *et al.* (LHCb Collaboration), Evidence of a $J/\psi\Lambda$ structure and observation of excited Ξ^- states in the $\Xi_b^- \to J/\psi\Lambda K^-$ decay, Sci. Bull. **66**, 1278 (2021).

[16] E. Kou *et al.* (Belle-II Collaboration), The Belle II physics book, Prog. Theor. Exp. Phys. **2019**, 123C01 (2019); Erratum, Prog. Theor. Exp. Phys. **2020**, 029201 (2020).

[17] R. N. Faustov and V. O. Galkin, Relativistic description of the Ξ_b baryon semileptonic decays, Phys. Rev. D **98**, 093006 (2018).

[18] C. Q. Geng, C. W. Liu, and T. H. Tsai, Nonleptonic two-body weak decays of Λ_b in modified MIT bag model, Phys. Rev. D **102**, 034033 (2020).

[19] C. Albertus, E. Hernandez, and J. Nieves, Nonrelativistic constituent quark model and HQET combined study of semileptonic decays of Λ_b and Ξ_b baryons, Phys. Rev. D **71**, 014012 (2005).

[20] D. Ebert, R. N. Faustov, and V. O. Galkin, Semileptonic decays of heavy baryons in the relativistic quark model, Phys. Rev. D **73**, 094002 (2006).

[21] H. Y. Cheng, Nonleptonic weak decays of bottom baryons, Phys. Rev. D **56**, 2799 (1997); Erratum, Phys. Rev. D **99**, 079901 (2019).

[22] M. A. Ivanov, J. G. Korner, V. E. Lyubovitskij, and A. G. Rusetsky, Exclusive nonleptonic bottom to charm baryon decays including nonfactorizable contributions, Mod. Phys. Lett. A **13**, 181 (1998).

[23] M. A. Ivanov, J. G. Korner, V. E. Lyubovitskij, and A. G. Rusetsky, Exclusive nonleptonic decays of bottom and charm baryons in a relativistic three quark model: Evaluation of nonfactorizing diagrams, Phys. Rev. D **57**, 5632 (1998).

[24] T. Gutsche, M. A. Ivanov, J. G. Körner, and V. E. Lyubovitskij, Nonleptonic two-body decays of single heavy baryons Λ_Q, Ξ_Q, and Ω_Q ($Q = b, c$) induced by W emission in the covariant confined quark model, Phys. Rev. D **98**, 074011 (2018).

[25] Z. X. Zhao, Weak decays of heavy baryons in the light-front approach, Chin. Phys. C **42**, 093101 (2018).

[26] C. K. Chua, Color-allowed bottom baryon to charmed baryon nonleptonic decays, Phys. Rev. D **99**, 014023 (2019).

[27] C. K. Chua, Color-allowed bottom baryon to s-wave and p-wave charmed baryon nonleptonic decays, Phys. Rev. D **100**, 034025 (2019).

[28] H. W. Ke, N. Hao, and X. Q. Li, Revisiting $\Lambda_b \to \Lambda_c$ and $\Sigma_b \to \Sigma_c$ weak decays in the light-front quark model, Eur. Phys. J. C **79**, 540 (2019).

[29] J. Zhu, Z. T. Wei, and H. W. Ke, Semileptonic and nonleptonic weak decays of Λ_b^0, Phys. Rev. D **99**, 054020 (2019).

[30] Y. S. Li, X. Liu, and F. S. Yu, Revisiting semileptonic decays of $\Lambda_{b(c)}$ supported by baryon spectroscopy, Phys. Rev. D **104**, 013005 (2021).

[31] Y. M. Wang, Y. Li, and C. D. Lu, Rare decays of $\Lambda_b \to \Lambda + \gamma$ and $\Lambda_b \to \Lambda\ell^+\ell^-$ in the light-cone sum rules, Eur. Phys. J. C **59**, 861 (2009).

[32] A. Khodjamirian, C. Klein, T. Mannel, and Y. M. Wang, Form factors and strong couplings of heavy baryons from QCD light-cone sum rules, J. High Energy Phys. 09 (2011) 106.

[33] Y. M. Wang and Y. L. Shen, Perturbative corrections to $\Lambda_b \to \Lambda$ form factors from QCD light-cone sum rules, J. High Energy Phys. 02 (**2016**) 179.

[34] Z. X. Zhao, R. H. Li, Y. L. Shen, Y. J. Shi, and Y. S. Yang, The semi-leptonic form factors of $\Lambda_b \to \Lambda_c$ and $\Xi_b \to \Xi_c$ in QCD sum rules, Eur. Phys. J. C **80**, 1181 (2020).

[35] P. Guo, H. W. Ke, X. Q. Li, C. D. Lu, and Y. M. Wang, Diquarks and the semi-leptonic decay of Λ_b in the hyrid scheme, Phys. Rev. D **75**, 054017 (2007).

[36] S. Capstick and N. Isgur, Baryons in a relativized quark model with chromodynamics, AIP Conf. Proc. **132**, 267 (1985).

[37] E. Hiyama and M. Kamimura, Study of various few-body systems using Gaussian expansion method (GEM), Front. Phys. **13**, 132106 (2018).

[38] E. Hiyama, Y. Kino, and M. Kamimura, Gaussian expansion method for few-body systems, Prog. Part. Nucl. Phys. **51**, 223 (2003).

[39] T. Yoshida, E. Hiyama, A. Hosaka, M. Oka, and K. Sadato, Spectrum of heavy baryons in the quark model, Phys. Rev. D **92**, 114029 (2015).

[40] G. Yang, J. Ping, P. G. Ortega, and J. Segovia, Triply heavy baryons in the constituent quark model, Chin. Phys. C **44**, 023102 (2020).

[41] S. Tawfiq, P. J. O'Donnell, and J. G. Korner, Charmed baryon strong coupling constants in a light front quark model, Phys. Rev. D **58**, 054010 (1998).

[42] S. Godfrey and N. Isgur, Mesons in a relativized quark model with chromodynamics, Phys. Rev. D **32**, 189 (1985).

[43] Q. T. Song, D. Y. Chen, X. Liu, and T. Matsuki, Charmed-strange mesons revisited: Mass spectra and strong decays, Phys. Rev. D **91**, 054031 (2015).

[44] C. Q. Pang, J. Z. Wang, X. Liu, and T. Matsuki, A systematic study of mass spectra and strong decay of strange mesons, Eur. Phys. J. C **77**, 861 (2017).

[45] J. Z. Wang, Z. F. Sun, X. Liu, and T. Matsuki, Higher bottomonium zoo, Eur. Phys. J. C **78**, 915 (2018).

[46] J. Z. Wang, D. Y. Chen, X. Liu, and T. Matsuki, Constructing J/ψ family with updated data of charmoniumlike Y states, Phys. Rev. D **99**, 114003 (2019).

[47] M. X. Duan and X. Liu, Where are 3P and higher P-wave states in the charmonium family?, Phys. Rev. D **104**, 074010 (2021).

[48] C. Chen, X. L. Chen, X. Liu, W. Z. Deng, and S. L. Zhu, Strong decays of charmed baryons, Phys. Rev. D **75**, 094017 (2007).

[49] B. Chen, S. Q. Luo, and X. Liu, Universal behavior of mass gaps existing in the single heavy baryon family, Eur. Phys. J. C **81**, 474 (2021).

[50] S. F. Biagi, M. Bourquin, A. J. Britten, R. M. Brown, H. J. Burckhart, A. A. Carter, C. Dore, P. Extermann, M. Gailloud, C. N. P. Gee *et al.*, Observation of a narrow state at 2.46 GeV/c^2: A candidate for the charmed strange Baryon A^+, Phys. Lett. **122B**, 455 (1983).

[51] P. L. Frabetti *et al.* (Fermilab E687 Collaboration), Measurement of the Mass and Lifetime of the Ξ_c^+, Phys. Rev. Lett. **70**, 1381 (1993).

[52] P. Avery *et al.* (CLEO Collaboration), Observation of the Charmed Strange Baryon Ξ_c^0, Phys. Rev. Lett. **62**, 863 (1989).

[53] R. Chistov *et al.* (Belle Collaboration), Observation of New States Decaying into $\Lambda_c^+ K^- \pi^+$ and $\Lambda_c^+ \to K_S^0 \pi^-$, Phys. Rev. Lett. **97**, 162001 (2006).

[54] S. F. Biagi, M. Bourquin, A. J. Britten, R. M. Brown, H. J. Burckhart, A. A. Carter, C. Doré, P. Extermann, M. Gailloud, C. N. P. Gee *et al.*, Properties of the charmed strange baryon $A+$ and evidence for the charmed doubly strange baryon T^0 at 2.74 GeV/c^2, Z. Phys. C **28**, 175 (1985).

[55] H. Albrecht *et al.* (ARGUS Collaboration), Evidence for the production of the charmed, doubly strange baryon Ω_c in e^+e^- annihilation, Phys. Lett. B **288**, 367 (1992).

[56] R. Aaij *et al.* (LHCb Collaboration), Observation of Five New Narrow Ω_c^0 States Decaying to $\Xi_c^+ K^-$, Phys. Rev. Lett. **118**, 182001 (2017).

[57] J. Yelton *et al.* (Belle Collaboration), Observation of excited Ω_c charmed baryons in e^+e^- collisions, Phys. Rev. D **97**, 051102 (2018).

[58] B. Chen and X. Liu, New Ω_c^0 baryons discovered by LHCb as the members of $1P$ and $2S$ states, Phys. Rev. D **96**, 094015 (2017).

[59] H. Y. Cheng and C. W. Chiang, Quantum numbers of Ω_c states and other charmed baryons, Phys. Rev. D **95**, 094018 (2017).

[60] H. X. Chen, Q. Mao, W. Chen, A. Hosaka, X. Liu, and S. L. Zhu, Decay properties of P-wave charmed baryons from light-cone QCD sum rules, Phys. Rev. D **95**, 094008 (2017).

[61] S. S. Agaev, K. Azizi, and H. Sundu, On the nature of the newly discovered Ω states, Europhys. Lett. **118**, 61001 (2017).

[62] K. L. Wang, L. Y. Xiao, X. H. Zhong, and Q. Zhao, Understanding the newly observed Ω_c states through their decays, Phys. Rev. D **95**, 116010 (2017).

[63] V. R. Debastiani, J. M. Dias, W. H. Liang, and E. Oset, $\Omega_b^- \to (\Xi_c^+ K^-)\pi^-$ and the Ω_c states, Phys. Rev. D **98**, 094022 (2018).

[64] H. Georgi, B. Grinstein, and M. B. Wise, Λ_b semileptonic decay form-factors for m_c does not equal infinity, Phys. Lett. B **252**, 456 (1990).

[65] K. C. Bowler, R. D. Kenway, L. Lellouch, J. Nieves, O. Oliveira, D. G. Richards, C. T. Sachrajda, N. Stella, and P. Ueberholz (UKQCD Collaboration), First lattice study of semileptonic decays of Λ_b and Ξ_b baryons, Phys. Rev. D **57**, 6948 (1998).

[66] C. D. Lu, Y. M. Wang, H. Zou, A. Ali, and G. Kramer, Anatomy of the pQCD approach to the baryonic decays $\Lambda_b \to p\pi, pK$, Phys. Rev. D **80**, 034011 (2009).

[67] R. Aaij *et al.* (LHCb Collaboration), Precision Measurement of the Mass and Lifetime of the Ξ_b^0 Baryon, Phys. Rev. Lett. **113**, 032001 (2014).

[68] R. Aaij *et al.* (LHCb Collaboration), Measurement of the Ξ_b^- and Ω_b^- baryon lifetimes, Phys. Lett. B **736**, 154 (2014).

[69] R. Aaij *et al.* (LHCb Collaboration), Measurement of the mass and lifetime of the Ω_b^- baryon, Phys. Rev. D **93**, 092007 (2016).

[70] T. A. Aaltonen *et al.* (CDF Collaboration), Mass and lifetime measurements of bottom and charm baryons in $p\bar{p}$ collisions at $\sqrt{s} = 1.96$ TeV, Phys. Rev. D **89**, 072014 (2014).

[71] H. Y. Cheng, C. K. Chua, and C. W. Hwang, Covariant light front approach for S wave and P wave mesons: Its application to decay constants and form-factors, Phys. Rev. D **69**, 074025 (2004).